Introduction of sulfate to stabilize the n = 3 Ruddlesden-Popper system Sr4Fe3O10-, as a potential SOFC cathode

Jarvis, Abbey; Berry, Frank; Marco, Jose F.; Slater, Peter

DOI:
10.1149/09101.1467ecst

Document Version
Peer reviewed version

Citation for published version (Harvard):
Jarvis, A, Berry, F, Marco, JF & Slater, P 2019, 'Introduction of sulfate to stabilize the n = 3 Ruddlesden-Popper system $Sr_4Fe_3O_{10-}$, as a potential SOFC cathode', *ECS Transactions*, vol. 91, no. 1, pp. 1467-1476. https://doi.org/10.1149/09101.1467ecst

Introduction of Sulfate to Stabilize the n = 3 Ruddlesden-Popper System $Sr_4Fe_3O_{10-\delta}$, as a Potential SOFC Cathode

A. Jarvis[a], F. J. Berry[a], J. F. Marco[b], and P. R. Slater[a]

[a] School of Chemistry, University of Birmingham, Birmingham B15 2TT, UK
[b] Instiuto de Quimica Fisica " Roscasolano", CSIC, Serrano 119, Madrid 28006, Spain

In this paper we report the successful incorporation of sulfate into the triple layer (n = 3) Ruddlesden-Popper system $Sr_4Fe_3O_{10-\delta}$, with characterisation of these materials by X-ray diffraction, Mössbauer spectroscopy, and conductivity measurements. Significantly, the incorporation of SO_4^{2-} into the middle perovskite layer leads to the stabilization of this Ruddlesden-Popper phase, which cannot be prepared without sulfate doping, thus highlighting the potential of oxyanion doping as a strategy to synthesise new phases of interest for solid oxide fuel cells.

Introduction

With increasing concerns regarding climate change due to the increased use of fossil fuels, alternate methods for electrical energy production are needed. Solid oxide fuel cells (SOFCs) are an appealing solution due to their high efficiency and consequent lower greenhouse gas emissions. Fuel cells have three main components, an anode, cathode and electrolyte, and research into all three components is being investigated in order to optimise performance while reducing cost.

Cathode materials for solid oxide fuel cells (SOFCs) are commonly systems with the perovskite structure, for example $La_{1-x}Sr_xMnO_3$ (LSM), which in addition to having high electronic conductivity is chemically compatible with the commonly used electrolyte yttria stabilized zirconia (YSZ) (1)–(3). More recently perovskite related Ruddlesden-Popper phases have been investigated as potential cathode materials for SOFCs. This is due to their appealing high mixed oxide and electronic conductivity, e.g. La_2NiO_4 (4),(5). Less widely studied are the n > 1 Ruddlesden-Popper systems. Related to the materials investigated in this paper, doped n = 2 Ruddlesden-Popper system, $Sr_3Fe_2O_{7-\delta}$ has been reported for use in SOFCs, with promising performance shown in conjunction with a proton conducting perovskite electrolyte (6)–(8). Ruddlesden-Popper systems have the general formula $A_{n+1}B_nO_{3n+1}$, where, as for perovskite systems, the A cation is large (e.g. alkaline earth/ rare earth element) and the B cation is small (e.g. a transition metal). Their structure consists of perovskite layers separated by rock salt layers, where the number of consecutive perovskite layers increases as n increases (Figure 1). An interesting aspect of these materials is their ability not only to accommodate anion vacancy defects within the perovskite layers, but also allow the incorporation of interstitial anions within the rock salt layers. Thus they have great flexibility for manipulating the composition and hence properties.

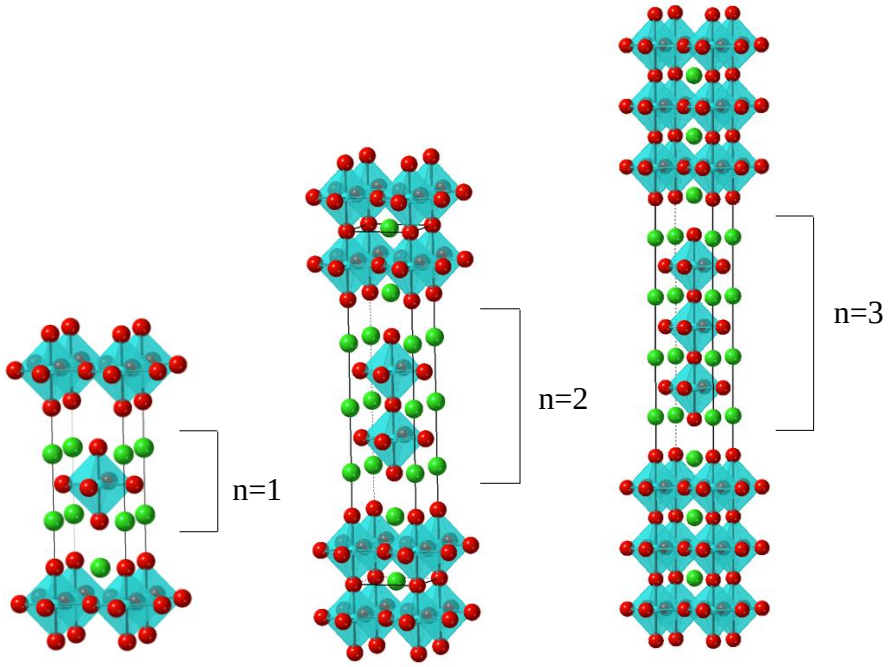

Figure 1. Structure of Ruddlesden-Popper type $A_{n+1}B_nO_{3n+1}$ systems: A (green), B (blue) and O (red)

As for perovskite systems, typical doping strategies for these materials have involved doping with cations of a different charge, but similar size. Recently the potential of alternative doping strategies with oxyanions (e.g. carbonate, borate (9), phosphate (9)–(14), silicate (15)–(18) and sulfate (10),(12),(19),(20)) has been shown in perovskite materials for the development of new solid oxide fuel cell materials. This doping strategy had previously been successfully applied to superconducting cuprate materials (21)–(30). A more detailed outline of oxyanion incorporation in perovskite materials can be found in the review article by Hancock *et al* (28).

Of relevance to the work presented here, we have recently shown that sulfate can be incorporated into the perovskite system $SrFeO_{3-\delta}$, leading to enhanced oxygen vacancy disorder under low $p(O_2)$ where the undoped system transforms to the oxygen vacancy ordered brownmillerite structure (31). Following on from these results we have investigated whether sulfate can be incorporated into the Ruddlesden-Popper system, $Sr_4Fe_3O_{10-\delta}$. Oxyanion incorporation in $Sr_4Fe_3O_{10-\delta}$ has previously been reported by Yamaura et al.(32) and Bréard et al (33). Specifically carbonate can be incorporated into $Sr_4Fe_3O_{10-\delta}$ to give the compound $Sr_4Fe_2O_6CO_3$. Furthermore Gonano et al.(34),(35) have recently reported the incorporation of carbonate and/or sulfate into the Ruddlesden-Popper system, $Sr_4Fe_3O_{10-\delta,}$ forming the materials $Sr_4Fe_{2.5}O_{7.25}(SO_4)_{0.5}$ and $Sr_4Fe_2[Fe_{0.5}(SO_4)_{0.25}(CO_3)_{0.25}]O_{7.25}$. Synthesis of these materials was, however, performed through solid state synthesis in evacuated sealed silica ampules. From an applications point of view, there is a need to determine whether synthesis in air is possible, and in this work we illustrate the successful incorporation of sulfate into $Sr_4Fe_3O_{10-\delta,}$ through standard solid state reaction in air. We also report preliminary studies on the conductivities of these sulfate doped phases, and stability in lower $p(O_2)$, with a view to evaluating their potential for use as cathodes in solid oxide fuel cells.

Experimental

The $Sr_4Fe_{3-x}S_xO_{10-\delta}$ phases were prepared through solid state synthesis using $SrCO_3$, Fe_2O_3 and $(NH_4)_2SO_4$. Samples were intimately ground and heated to 950 °C (4 °C/ min) for 12 hours after which samples were ball milled (350 rpm for 1 h, Fritsch Pulverisette 7 planetary Mill, zirconia balls and container) and reheated to 1000 °C. A further grinding of the samples was carried out before heating to 1050 °C for 12 hours. Finally, samples were annealed at 350 °C for 12 h in air in order to ensure maximum oxygen content. Additionally, samples were heated in N_2 in order to test their stability under lower $p(O_2)$. Samples were heated to 800 °C for 12 h with a ramp rate of 4 °C/ min.

Powder X-ray diffraction (Panalytical Empyrean diffractometer equipped with a Pixcel 2D detector (Cu Kα radiation)) was used to determine lattice parameters and phase purity. Rietveld refinements were carried out by using the GSAS suite of programs (36). Space group I4/mmm was used for all these Ruddlesden-Popper samples with an additional cubic perovskite phase (Pm-3m) included as a minor impurity.

The ^{57}Fe Mössbauer spectra was carried out at 298 K in constant acceleration mode using approximately 25 mCi Co/Rh source.

Four probe dc conductivity measurements were carried out for all samples: powders were ball milled (350 rpm for 1 h, Fritsch Pulverisette 7 planetary Mill), before pressing into pellets and sintering at 1050 °C for 12 h. Pt electrodes were attached to the pellets with Pt paste before heating to 900 °C for 1 h to ensure good contact. The pellets were finally annealed at 350 °C for 12 h.

Results and Discussion

X-ray Diffraction

X-ray diffraction (XRD) studies for the $Sr_4Fe_{3-x}S_xO_{10-\delta}$ systems indicated that upon doping with sulfate the n = 3 Ruddlesden-Popper structure is formed for x = 0.15 - 0.3 (Figure 2). In comparison when attempting to synthesise the undoped $Sr_4Fe_3O_{10-\delta}$ system, an impure sample is formed which is a mixture of $Sr_3Fe_2O_{7-\delta}$ and $SrFeO_{3-\delta}$. This can be more clearly seen in Figure 2b for the range $2\theta \approx 40 - 45°$, where a significant difference in the XRD patterns can be observed between the undoped (x = 0) and the sulfate doped samples. Thus sulfate is shown to successfully stabilize the n = 3 Ruddlesden-Popper system, further illustrating the potential of oxyanion doping to design new potential SOFC materials.

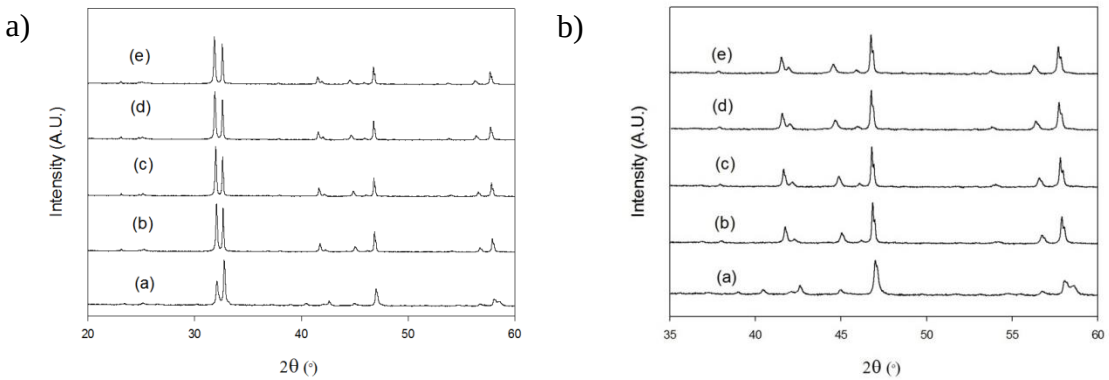

Figure 2. (a) X-ray diffraction patterns for $Sr_4Fe_{3-x}S_xO_{10-\delta}$ where a) x = 0, b) x = 0.15, c) x = 0.2, d) x = 0.25 and e) x = 0.3. (b) Expanded region to illustrate differences between x = 0, and x > 0 samples.

Using the XRD data, Rietveld refinements were performed on samples, both as prepared and after heating in N_2 (an example fit is shown in Figure 3). The initial refinements indicated a low Fe occupancy in the middle perovskite layer consistent with partial SO_4^{2-} in this layer. Adding S to this site and refining the Fe/S occupancies (with the constraint that the total occupancy was 1) gave good agreement with the expected values (TABLE I). Due to asymmetric broadening in the X-ray diffraction data, uniaxial strain was included. A possible explanation for the asymmetric broadening could be the presence of stacking faults along [001], which is common for Ruddlesden-Popper systems (37). A small amount (< 2.5 wt%) of perovskite impurity was also included in the final refinement.

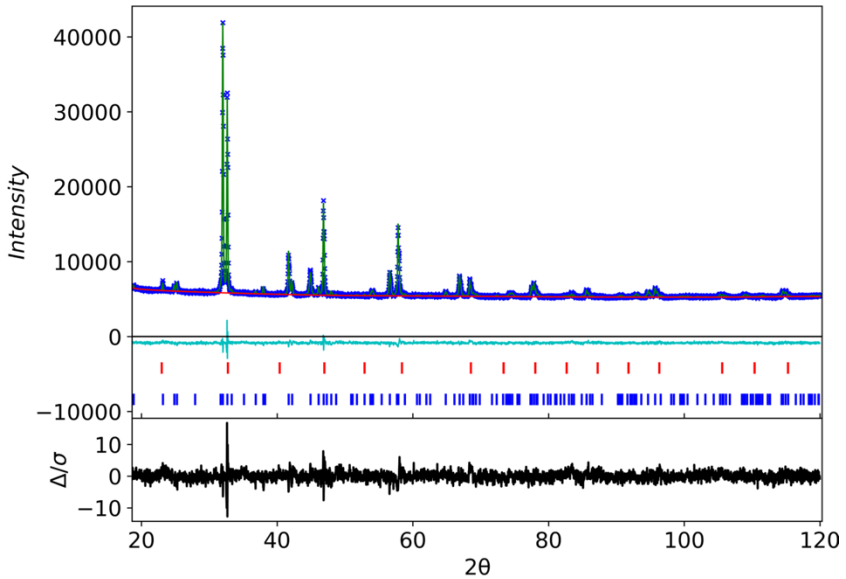

Figure 3. Observed, calculated and difference X-ray diffraction profiles for $Sr_4Fe_{2.8}S_{0.2}O_{10-\delta}$. The two phases are indicated by blue (Ruddlesden-Popper, I4/mmm) and red ticks (perovskite Pm-3m)

From the calculated lattice parameters, it can be seen that there is an approximate linear increase between x = 0.15 - 0.25 (Figure 4). The linear trend does not continue for x = 0.3, suggesting the solubility limit of sulfate in the structure is between x = 0.25 and

0.3. While at first glance this increase in cell volume might be surprising given the smaller size of S^{6+} compared to Fe^{3+}/ Fe^{4+}, it can be correlated with an increase in the proportion of the larger Fe^{3+} upon doping with sulfate (confirmed by ^{57}Fe Mössbauer spectroscopy (see later)). Similar cell expansions due to reduction in the average oxidation state of the transition metal on oxyanion doping has been observed in related perovskite systems (31). This can be correlated with the sulfate group helping to stabilize oxide ion vacancy defects.

In addition to sulfate doping, phosphate doping of $Sr_4Fe_3O_{10-\delta}$ was also investigated. However this dopant did not give the desired n = 3 Ruddlesden-Popper system, but rather a mixture of $Sr_3Fe_2O_{7-\delta}$, $SrFeO_{3-\delta}$, $Sr_5(PO_4)_3(OH)$ and $SrCO_3$ was formed.

TABLE I. Lattice parameters (space group I4/mmm) and middle Fe layer site occupancy factors for $Sr_4Fe_{3-x}S_xO_{10-\delta}$ (heating in air). The impurity phase, $SrFeO_{3-\delta}$, was refined in the cubic space group, Pm-3m

		$Sr_4Fe_{3-x}S_xO_{10-\delta}$			
S (x)		0.15	0.2	0.25	0.3
a (Å)		3.8735(1)	3.8768(1)	3.8793(1)	3.8787(1)
c (Å)		28.1682(7)	28.2444(6)	28.3476(7)	28.3682(10)
V (Å^3)		422.64(2)	424.49(2)	426.60(2)	426.77(3)
Rwp (%)		1.80	1.71	1.74	1.97
Rexp (%)		1.30	1.29	1.31	1.30
Fe occupancy (middle perovskite layer)		0.82(3)	0.81(3)	0.73(3)	0.66(4)
S occupancy (middle perovskite layer)		0.18(3)	0.19(3)	0.27(3)	0.34(4)
Perovskite ($SrFeO_3$)	a (Å)	3.8638(4)	3.8659(4)	3.8816(4)	3.8725(3)
	V (Å^3)	57.68(2)	57.78(2)	58.48(2)	58.07(2)
Weight percentage (%)	Ruddlesden-Popper	98.3	98.6	97.9	97.6
	Perovskite	1.7	1.4	2.1	2.4

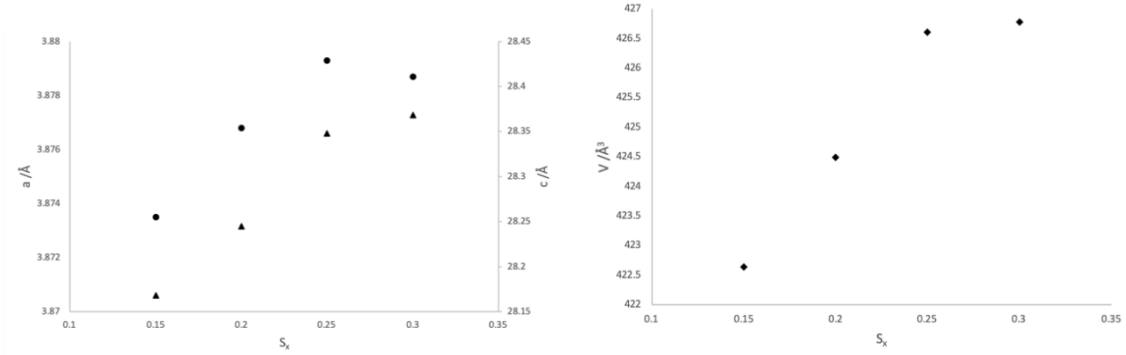

Figure 4. Plots of lattice parameters vs x ($Sr_4Fe_{3-x}S_xO_{10-\delta}$), where a = ●, c = ▲ and V = ◆

Stability in Lower p(O_2)

The stability of $Sr_4Fe_{3-x}S_xO_{10-\delta}$ samples were tested in N_2 to 800 °C. The results indicated that these n = 3 Ruddlesden-Popper phases appear to remain stable (Figure 5) for the sulfate doped phases, x = 0.2 - 0.3. For lower levels of sulfate some small changes are observed in the XRD patterns (Figure 5). This might be due to the partial break down of the structure to produce the n = 2 Ruddlesden-Popper system, $Sr_3Fe_2O_{7-\delta}$, and further work is required to investigate this.

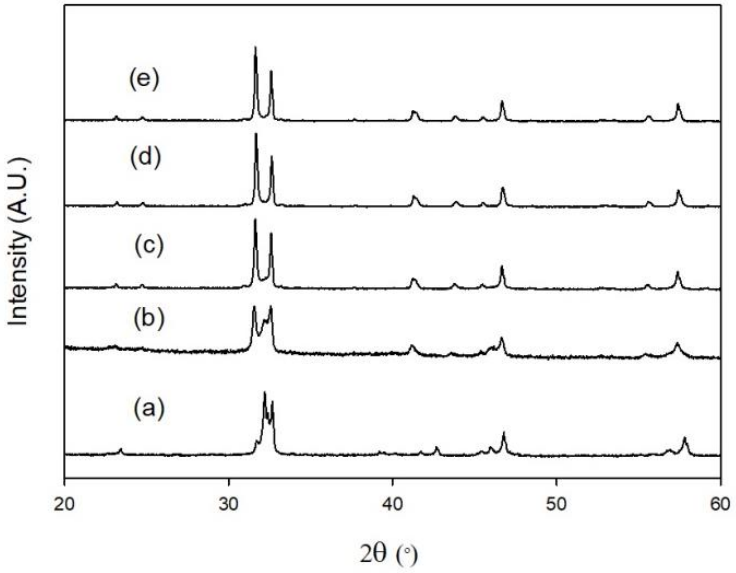

Figure 5. X-Ray diffraction patterns for $Sr_4Fe_{3-x}S_xO_{10-\delta}$ after heat treatment in N_2 to 800 °C, where a) x = 0, b) x = 0.15, c) x = 0.2, d) x = 0.25 and e) x = 0.3. Results show significant changes for $x \leq 0.15$.

Overall an increase in lattice parameters is observed for the N_2 treated samples compared to the samples synthesised in air. This is as predicted due to the reduction of Fe^{4+} to the larger Fe^{3+} which can be seen by the change in colour of samples from black to brown. For these N_2 treated samples, we now see the expected general decrease in cell volume with sulfate content (due to the smaller size of S^{6+} versus Fe^{3+}), as the Fe oxidation state is now the same (3+) in each sample.

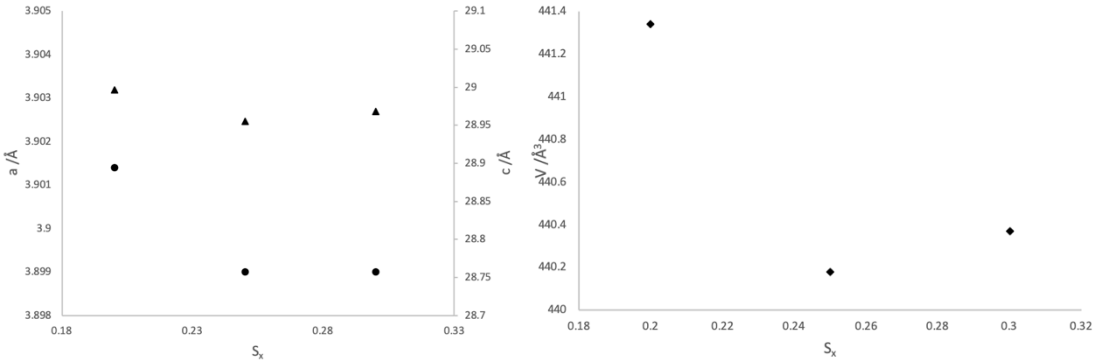

Figure 6. Plots of lattice parameters vs x ($Sr_4Fe_{3-x}S_xO_{10-\delta}$ samples N_2 to 800°C), where a = ●, c = ▲ and V = ◆

Conductivity Data

The conductivity data for the $Sr_4Fe_{3-x}S_xO_{10-\delta}$ samples, showed generally similar values for all samples (Figure 7). When comparing the conductivities of these Ruddlesden-Popper $Sr_4Fe_{3-x}S_xO_{10-\delta}$ samples with our previous results for perovskite-type $SrFe_{1-x}S_xO_{3-\delta}$ (31), the results show that higher conductivities are observed for the latter.

This generally low electronic conductivity may be a problem for the utilization of these systems as SOFC cathodes. However, it is likely that doping with other transition metals, e.g. Co, may lead to an enhancement of the conductivity, which is a future avenue of research.

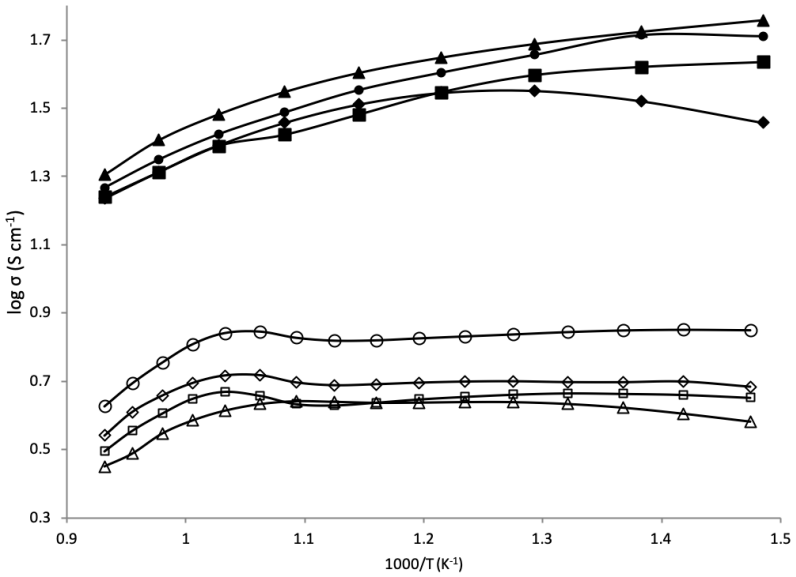

Figure 7. Plot of log σ vs. 1000/T for $Sr_4Fe_{3-x}S_xO_{10-\delta}$ where x = 0.15 (○), 0.2 (□), 0.25 (△), 0.3 (◇) and $SrFe_{1-x}S_xO_{3-\delta}$ (31) where x = 0 (●), 0.025 (■), 0.05 (▲), 0.075 (◆) in air

^{57}Fe Mossbauer Spectroscopy

^{57}Fe Mössbauer spectroscopy was carried out at 298 K for $Sr_4Fe_{2.85}S_{0.15}O_{10-\delta}$ and $Sr_4Fe_{2.7}S_{0.3}O_{10-\delta}$ (Figure 8 & TABLE II). Previous studies of the perovskite system, $SrFeO_{3-\delta}$, reported chemical isomer shifts of $\delta \approx 0.15$ and 0.05 mm s^{-1} which are assigned to $Fe^{3.5+}$ and Fe^{4+} respectively (38)–(40). In other work disproportionation of Fe^{4+} to $Fe^{3+}$and Fe^{5+} is observed for both Si^{4+} and Sn^{4+} doping of $SrFeO_{3-\delta}$ (15),(41). In the case of silicon doping of $SrFeO_{3-\delta}$, disproportionation of Fe^{4+} to Fe^{3+} ($\delta \approx 0.37$ mm s^{-1}) and Fe^{5+} ($\delta \approx -0.05$ mm s^{-1}) occurs with the addition of some of the Fe^{3+} in lower than octahedral coordination ($\delta \approx 0.18$ mm s^{-1}) (15). In addition to the perovskite systems, disproportionation of Fe^{4+} is also observed in the Ruddlesden-Popper system, $Sr_4Mn_{3-x}Fe_xO_{10-\delta}$ (42).

Using the assignments described for the above perovskite and Ruddlesden-Popper systems, chemical isomer shifts $\delta \approx -0.02$ and 0.28/0.30 mm s^{-1} ($S_{0.15}$/ $S_{0.3}$) can be assigned to Fe^{5+} and Fe^{3+} respectively. Furthermore the chemical isomer shifts $\delta \approx 0.23$ mm s^{-1} ($S_{0.15}$) and 0.24/0.16 mm s^{-1} ($S_{0.3}$) can be assigned to Fe^{3+} in lower than octahedral coordination. This has previously been reported in $SrFe_{1-x}Si_xO_{3-\delta}$, where it has been reported that the substitution of the smaller Si^{4+} for Fe^{4+} results in the surrounding of Si^{4+} with the larger Fe^{3+} (15). As a result it has been suggested that local strain is introduced which is relieved by incorporating Fe^{5+}. A similar effect therefore appears to be present in these Ruddlesden-Popper systems, $Sr_4Fe_{3-x}S_xO_{10-\delta}$. Overall the data indicate that the amount of Fe^{3+} increases with sulfate content, which can be correlated with increased

oxide ion vacancy defect incorporation and the observed increase in lattice parameters with increased sulfate content as previously discussed.

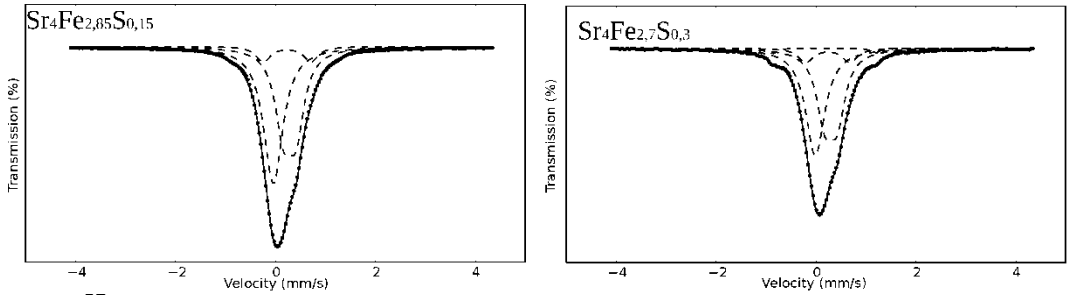

Figure 8. ^{57}Fe Mössbauer spectrum from $Sr_4Fe_{2.85}S_{0.15}O_{10-\delta}$ and $Sr_4Fe_{2.7}S_{0.3}O_{10-\delta}$ at 298 K

TABLE II. ^{57}Fe Mössbauer parameters recorded from $Sr_4Fe_{2.85}S_{0.15}O_{10-\delta}$ and $Sr_4Fe_{2.7}S_{0.3}O_{10-\delta}$ at 298 K

Compound	**Assignment**	**δ ± 0.01 (mms^{-1})**	**Δ ± 0.05 (mms^{-1})**	**Area ± 5% (%)**
$Sr_4Fe_{2.85}S_{0.15}O_{10-\delta}$	Fe^{5+}	-0.02	X	59
	Fe^{3+}	0.28	0.28	34
	Fe^{3+} in low coordination	0.23	0.91	7
$Sr_4Fe_{2.7}S_{0.3}O_{10-\delta}$	Fe^{5+}	-0.02	0.00	44
	Fe^{3+}	0.30	0.24	45
	Fe^{3+} in low coordination	0.24	0.90	9
		0.16	2.04	2

Conclusion

The present study demonstrates that sulfate can successfully be incorporated into the n = 3 Ruddlesden-Popper structure, $Sr_4Fe_3O_{10-\delta}$, allowing this phase to be successfully stabilized and hence synthesised (without sulfate, a mixture of n = 2 Ruddlesden-Popper and perovskite phases is observed). The successful synthesis is most likely related to the stabilization of oxide ion vacancies by the sulfate, as previously proposed as key for other oxyanion doping of perovskite and related systems (28). Although the conductivities are lower than sulfate doped perovskite $SrFeO_{3-\delta}$, the results further highlight the potential of oxyanion doping as a strategy to synthesise new phases of interest for solid oxide fuel cells. Further work will investigate enhancing the conductivity through Co doping as well as the ability of these materials to accommodate water and hence display mixed electronic and protonic conductivity with a view to possible use in conjunction with a proton conducting electrolyte, as for the n = 2 system (6-8).

Acknowledgments

We would like to thank the University of Birmingham and EPSRC for funding (studentship for AJ). The authors also thank EPSRC for funding: the JUICED Hub (Joint University Industry Consortium for Energy (Materials) and Devices Hub), EP/R023662/1).

Raw experimental data can be found at: https://doi.org/10.25500/edata.bham.00000341.

References

1. Mizusaki, J. and Sasamoto, T., *J. Am. Ceram. Soc.*, **66**, 247 (1983).
2. Kamata, H., Yonemura, Y., Mizusaki, J., Tagawa, H., Naraya, K., and Sasamoto, T. i., *J. Phys. Chem. Solids*, **56**, 943 (1995).
3. Anderson, H. U., Sparlin, D. M., Lamno, T., and Lamno, S., *J. Solid State Chem.*, **87**, 55 (1990).
4. Skinner, S. J. and Kilner, J. A., *Solid State Ionics*, **135**, 709 (2000).
5. Amow, G. and Skinner, S. J., *J. Solid State Electrochem.*, **10**, 538 (2006).
6. Samain, L., Amshoff, P., Biendicho, J. J., Tietz, F., Mahmoud, A., Hermann, R. P., Istomin, S. Y., Grins, J., and Svensson, G., *J. Solid State Chem.*, **227**, 45 (2015).
7. Wang, Z., Yang, W., Shafi, S. P., Bi, L., Wang, Z., Peng, R., Xia, C., Liu, W., and Lu, Y., *J. Mater. Chem. A*, **3**, 8405 (2015).
8. Huan, D., Wang, Z., Wang, Z., Peng, R., Xia, C., and Lu, Y., *ACS Appl. Mater. Interfaces*, **8**, 4592 (2016).
9. Porras-Vazquez, J. M., Kemp, T. F., Hanna, J. V., and Slater, P. R., *J. Mater. Chem.*, **22**, 8287 (2012).
10. Shin, J. F., Orera, A., Apperley, D. C., and Slater, P. R., *J. Mater. Chem.*, **21**, 874 (2011).
11. Shin, J. F., Hussey, L., Orera, A., and Slater, P. R., *Chem. Commun.*, **46**, 4613 (2010).
12. Hancock, C. A., Slade, R. C. T., Varcoe, J. R., and Slater, P. R., *J. Solid State Chem.*, **184**, 2972 (2011).
13. Li, M., Zhou, W., Xu, X., and Zhu, Z., *J. Mater. Chem. A*, **1**, 13632 (2013).
14. Zhu, Y., Zhou, W., Sunarso, J., Zhong, Y., and Shao, Z., *Adv. Funct. Mater.*, **26**, 5862 (2016).
15. Porras-Vazquez, J. M., Pike, T., Hancock, C. A., Marco, J. F., Berry, F. J., and Slater, P. R., *J. Mater. Chem. A*, **1**, 11834 (2013).
16. Porras-Vazquez, J. M., Smith, R. I., and Slater, P. R., *J. Solid State Chem.*, **213**, 132 (2014).
17. Shin, J. F., Apperley, D. C., and Slater, P. R., *Chem. Mater.*, **22**, 5945 (2010).
18. Hancock, C. A. and Slater, P. R., *Dalton Trans.*, **40**, 5599 (2011).
19. Liu, Y., Zhu, X., and Yang, W., *J. Memb. Sci.*, **501**, 53 (2016).
20. Pérez-Coll, D., Pérez-Flores, J. C., Nasani, N., Slater, P. R., and Fagg, D. P., *J. Mater. Chem. A*, **4**, 11069 (2016).
21. Slater, P. R., Greaves, C., Slaski, M., and Muirhead, C. M., *Phys. C Supercond. its Appl.*, **208**, 193 (1993).
22. Francesconi, M. G. and Greaves, C., *Supercond. Sci. Technol.*, **10**, A29 (1997).
23. Maignan, A., Pelloquin, D., Malo, S., Michel, C., Hervieu, M., and Raveau, B., *Phys. C Supercond.*, **249**, 220 (1995).
24. Goutenoire, F., Hervieu, M., Maignan, A., Michel, C., Martin, C., and Raveau, B., *Phys. C Supercond.*, **210**, 359 (1993).
25. Kinoshita, K. and Yamada, T., *Nature*, **357**, 313 (1992).
26. Huvé, M., Michel, C., Maignan, A., Hervieu, M., Martin, C., and Raveau, B., *Phys. C Supercond. its Appl.*, **205**, 219 (1993).
27. Letouzé, F., Martin, C., Maignan, A., Michel, C., Hervieu, M., and Raveau, B.,

Phys. C Supercond., **254**, 33 (1995).
28. Hancock, C. A., Porras-Vazquez, J. M., Keenan, P. J., and Slater, P. R., *Dalt. Trans.*, **44**, 10559 (2015).
29. Speakman, S. A., Richardson, J. W., Mitchell, B. J., and Misture, S. T., *Solid State Ionics*, **149**, 247 (2002).
30. Starkov, I., Bychkov, S., Matvienko, A., and Nemudry, A., *Phys. Chem. Chem. Phys.*, **16**, 5527 (2014).
31. Jarvis, A. and Slater, P. R., *Crystals*, **7**, 169 (2017).
32. Yamaura, K., Huang, Q., Lynn, J. W., Erwin, R. W., and Cava, R. J., *J. Solid State Chem.*, **152**, 374 (2000).
33. Breard, Y., Michel, C., Hervieu, M., and Raveau, B., *J. Mater. Chem.*, **10**, 1043 (2000).
34. Gonano, B., Bréard, Y., Pelloquin, D., Caignaert, V., Perez, O., Pautrat, A., Boullay, P., Bazin, P., and Le Breton, J.-M., *Inorg. Chem.*, **56**, 15241 (2017).
35. Gonano, B., Bréard, Y., Pelloquin, D., Caignaert, V., Pérez, O., Pautrat, A., Bazin, P., Suard, E., and Boullay, P., *Dalt. Trans.*, **47**, 13088 (2018).
36. Toby, B. H. and Von Dreele, R. B., *J. Appl. Crystallogr.*, **46**, 544 (2013).
37. Seshadri, R., Hervieu, M., Martin, C., Maignan, A., Domenges, B., Raveau, B., and Fitch, A. N., *Chem. Mater.*, **9**, 1778 (1997).
38. Berry, F. J., Ren, X., Heap, R., Slater, P., and Thomas, M. F., *Solid State Commun.*, **134**, 621 (2005).
39. Berry, F. J., Heap, R., Helgason, Ö., Moore, E. A., Shim, S., Slater, P. R., and Thomas, M. F., *J. Phys. Condens. Matter*, **20** (2008).
40. Adler, P., Lebon, A., Damljanović, V., Ulrich, C., Bernhard, C., Boris, A. V., Maljuk, A., Lin, C. T., and Keimer, B., *Phys. Rev. B*, **73**, 094451 (2006).
41. Berry, F. J., Bowfield, A. F., Coomer, F. C., Jackson, S. D., Moore, E. A., Slater, P. R., Thomas, M. F., Wright, A. J., and Ren, X., *J. Phys. Condens. Matter*, **21**, 256001 (2009).
42. Fawcett, I. D., Veith, G. M., Greenblatt, M., Croft, M., and Nowik, I., *J. Solid State Chem.*, **155**, 96 (2000).